Innovative Food Science and Emerging Technologies 81 (2022) 103121

Contents lists available at ScienceDirect

Innovative Food Science and Emerging Technologies

journal homepage: www.elsevier.com/locate/ifset

Efficacy of cold atmospheric plasma for inactivation of viruses on raspberries

Branko Velebit [a,*], Lazar Milojević [a], Tatjana Baltić [a], Nevena Grković [b], Sanjay Gummalla [c], Marina Velebit [d], Ines Škoko [e], Sandra Mojsova [f], Predrag Putnik [g]

[a] Institute of Meat Hygiene and Technology, Kaćanskog 13, 11040 Belgrade, Serbia
[b] Faculty of Veterinary Medicine, University of Belgrade, Bulevar oslobođenja 18, 11000 Belgrade, Serbia
[c] American Frozen Food Institute, 2345 Crystal Drive, Arlington, VA 2220, USA
[d] Chemical Agrosava, Palmira Toljatija 5/IV, 11070 Belgrade, Serbia
[e] Croatian Veterinary Institute, Veterinary Department Split, Poljička cesta 33, 21000 Split, Croatia
[f] Faculty of Veterinary Medicine, Ss. Cyril and Methodius University in Skopje, St. "Lazar Pop-Trajkov" 5-7, 1000 Skopje, North Macedonia
[g] University North, Trg dr. Žarka Dolinara 1, 48000 Koprivnica, Croatia

ARTICLE INFO

Keywords:
Norovirus
Hepatitis A virus
Cold plasma
Inactivation
Raspberries

ABSTRACT

In this study, the effectiveness of cold atmospheric plasma (CAP) in inactivating murine norovirus (MNV/human norovirus surrogate) and hepatitis A virus (HAV) on aerosol-inoculated dark red Willamette raspberries was explored. Pulsed positive corona discharge system fed by synthetic air was used for the production of CAP. Raspberries were treated for 1, 3, 5, 7, and 10 min at 25 W. Application of CAP enabled a 4 $\log_{10}$ infectivity reduction in <5 min for MNV and approximately 10 min for HAV (from starting level of 6.91 and 7.84 $\log_{10}$ PFU/mL, respectively). Viral genome copies reduction of 3.18 $\log_{10}$ for MNV and 4.32 for HAV were found from starting level of 5.76 and 6.47 $\log_{10}$ gc/μL, respectively. CAP treatment did not result in significant degradation of fruit color, an important quality attribute. The study demonstrated CAP as an efficient post-harvest decontamination method to reduce viral load in raspberries without significantly affecting its quality parameters.

Industrial relevance: Due to the fast-processing paces required in the raspberry industry, it is difficult to assure the complete microbiological safety of this fruit. Cold atmospheric plasma is a practical, environmentally-friendly, non-thermal tool for the effective reduction of microbial pathogens. The model developed in this study demonstrated that CAP treatment of fresh raspberries not only inactivated hazardous enteric viruses in a short time (10 min) but also unaffected fruit color stability. The simplicity of described CAP design and low-cost inputs (air and electricity) enable the commercial application of inexpensive plasma chambers for continuous surface decontamination of large volumes of raspberries without bringing processing to a standstill.

1. Introduction

Raspberries (*Rubus idaeus* L.) belong to a group of soft red fruits of extraordinary nutritional composition, which render a range of health benefits. Popularity and consumption of this fruit significantly increased in recent years due to the rise of discretionary incomes in Europe and North America, increased urbanization, and new eating preferences. However, in the past two decades, the brambles (a group of fruits commonly comprised of raspberries and blackberries) have been implicated in an increasingly greater number of foodborne outbreaks associated with the consumption of contaminated fresh and frozen fruit (Dewey-Mattia, Manikonda, Hall, Wise, & Crowe, 2018; Tavoschi et al., 2015).

Human norovirus (HuNoV) and Hepatitis A virus (HAV) were identified as the dominant causative agents responsible for these outbreaks (Sánchez & Bosch, 2016; WHO, 2019). HuNoV is a highly contagious, small (27–38 nm), non-enveloped, single-stranded positive-RNA virus, classified into the *Caliciviridae* family. The clinical course of HuNoV infection is usually mild, and the most common symptoms are vomiting, acute gastroenteritis, diarrhea, nausea, and abdominal pain while people heal naturally within 1 to 3 days (Ryu, 2017). HAV is also a small (27–35 nm), non-enveloped single-stranded RNA virus of the *Picornaviridae* family. In HAV infection clinical symptoms develop after 14–28 days (up to 50 days). In adults, common symptoms are fever, nausea,

* Corresponding author.
E-mail address: branko.velebit@inmes.rs (B. Velebit).

https://doi.org/10.1016/j.ifset.2022.103121
Received 25 April 2022; Received in revised form 12 August 2022; Accepted 18 August 2022
Available online 23 August 2022

diarrhea, loss of appetite, jaundice and dark-colored urine, and occasionally acute fulminant hepatitis. The elderly population (> 65 years of age) is extremely vulnerable and at the highest risk for death from HuNoV and HAV infection (Cardemil, Parashar, & Hall, 2017; Ohfuji et al., 2019).

HuNoV and HAV are primarily transmitted via the fecal-oral route through contact with infected persons or uptake of raw or poorly cooked contaminated food (shellfish, fruit, vegetables) and water, where the virus can remain infectious for years. Berries are usually contaminated during pre-harvest, for example by sewage water pollution during growth, or post-harvest, for example via infected food handlers or fecally contaminated equipment (Rutjes, van den Berg, Lodder, & de Roda Husman, 2006). Because they only require a small inoculum to trigger an infection (< 100 virions), are pathogenic, and have the ability to survive in different environments, HuNoV and HAV are responsible for a significant burden of foodborne illnesses worldwide. As reported in previous summaries (CDC, 2021; Dewey-Mattia et al., 2018), HuNoV is the leading cause of foodborne disease outbreaks and outbreak-associated illnesses in the United States. Among 2953 outbreaks (2009–2015) with a single confirmed etiology, HuNoV was the most common cause of outbreaks (1130 outbreaks [38%]) and outbreak-associated illnesses (27,623 illnesses [41%]). Most foodborne norovirus outbreaks in the U.S. are associated with ready-to-eat foods contaminated during preparation by infected food workers in food service settings such as schools, nursing homes, hospitals, cruise ships, and catered events (Dewey-Mattia et al., 2018). Contaminated raw food products, specifically fresh and frozen fruit, leafy vegetables, and mollusks, have been implicated in norovirus outbreaks; thus, indicating upstream contamination during production. A similar trend occurred in the European Union. Namely, in 2019, HuNoV was the second most frequently reported causative agent in foodborne outbreaks in the EU and was reported by 21 Member States (EFSA, 2021). HuNoV was associated with 457 outbreaks and, most importantly, with 11,125 related illnesses (22.5% of total cases) meaning one in five of all outbreak-related illnesses in the EU. A fair number of HuNoV outbreaks were associated with the consumption of contaminated fruits and juice, in particular, frozen and fresh berries, pre-cut melon, and dates (EFSA, 2021). Large and prolonged multistate hepatitis A outbreak associated with the consumption of berries occurred in 2013 in the EU (Severi et al., 2015).

Regulatory agencies across the world have set high hygienic standards and recommend various control strategies for the prevention and control of pathogenic microorganisms in raspberries and the production and processing environments. There are, however, no effective treatments that are currently available for non-thermal pathogen inactivation that can be applied to the berries themselves. Raspberries are characterized by fragile and thin skin, thus rendering them sensitive to UV treatment (causing fruit discoloration) and at the same time tend to absorb moisture and attract mold growth.

Cold atmospheric plasma (CAP) is partially ionized, near-room temperature gas, produced at atmospheric pressure by applying high electric alternate or direct currents, radio frequencies, or microwaves between electrodes surrounded by gas and composed of a reactive mix of electrons, ions, excited atoms and molecules, reactive species, weak UV radiation, and low heat. CAP technology relies on various types of plasma sources such as jet plasma, dielectric barrier discharge (DBD) plasma, and corona discharge plasma. Although the DBD design setup has been widely used in CAP production, a pulsed corona discharge plasma (PCDP) design has also attracted considerable interest in cold plasma antimicrobial treatment because of its high removal efficiency and environmental compatibility (Song et al., 2022; Xin, Li, Lei, & Yang, 2016). During the PCDP treatment process, numerous reactive oxygen-based species – ROS (superoxide, hydroxyl radical, singlet oxygen, ozone) and/or nitrogen-based species – RNS (nitric oxide, nitrogen dioxide, and peroxynitrite) are generated which in combination with the UV light efficiently eliminate microorganisms (Song et al., 2022).

Both types of reactive species trigger various pathogen inactivation mechanisms, such as denaturation of the viral capsid protein, oxidation of amino acids, and irreversible denaturation of nucleic acids. The efficacy of CAP depends on the pathogen type, physical and chemical properties of the food matrix, operating gas mixture, and flow rate (Aboubakr, Sampedro Parra, Collins, Bruggeman, & Goyal, 2020). Aboubakr et al. (2018) demonstrated that ROS and RNS produced by CAP block virus adhesion and entry into host cells, by oxidation of amino acids of the VP1 domain (in the region of the N-terminal arm, shell domain, protrusion domain) and damage the capsid protein. Ahlfeld et al. (2015) and Bunz, Mese, Zhang, Piwowarczyk, and Ehrhardt (2018) also showed that cold plasma has virucidal effects on foodborne viruses (e.g., MNV, HAV, HuNoV, adenovirus). A study by Pradeep and Chulkyoon (2016) indicated that CAP acts on the surface of food and can modify or degrade viral proteins, nucleic acids, and lipids in enveloped viruses. It should be noted that the inactivation of viruses by various processing techniques does not follow a linear inactivation model (first-order kinetics), which assumes a linear logarithmic reduction of the quantity of the treated virus with time (Bozkurt, D'Souza, & Davidson, 2015a). A virus inactivation curve typically demonstrates a shouldering and tailing at the beginning and end of the curve, respectively, which limits the usage of decimal reduction times (D values) to establish the inactivation parameters (Araud et al., 2016). Consequently, alternative models, such as the Weibull model or biphasic reduction model are used for the estimation of virus survival (Tuladhar, Bouwknegt, Zwietering, Koopmans, & Duizer, 2012.).

In addition to high efficiency without heat treatment, CAP sanitization is characterized by short treatment time at ambient temperature and relatively low cost (Liao et al., 2017). The method is also environmentally friendly because it is not only chemical- and water-free but also, unlike chlorine-based treatments, cold plasma processes leave no harmful residues (Niemira, 2012; Pexara & Govaris, 2020). According to the report of the European Commission from 2014, CAP is allowed as an electronic method for preserving organic food (EC, 2014). From the berry fruit industry's perspective, these advantages position CAP technology as an effective microbial reduction technique against foodborne viruses while preserving the fruit's important sensory and nutritional characteristics. Information on CAP application to reduce foodborne viruses and their surrogates in berries is scarce and needs further exploration.

The objective of this study was to evaluate the efficacy of cold atmospheric plasma inactivation against human norovirus surrogate (MNV) and HAV in raspberries. To demonstrate empirical evidence for an antiviral effect on viral capsid integrity and viral genomes, we have employed a combination of three independent methods (RT-qPCR assay, transmission electron microscopy, and cell culture-based infectivity assays). In addition, we have evaluated the impact of CAP treatment on fruit color and consumer acceptance.

2. Materials and methods

2.1. Raspberry samples

Raspberries (*Rubus idaeus* L., cv. Willamette) were obtained from Ecocert Organic Standard-certified orchard in Western Serbia (geographic coordinates 43°40′12.1"N, 20°11′31.5″E). All berries were collected by hand during mid-July, supervised by the Chief agronomist. Only raspberries of a uniform degree of maturity were sampled. The maturity criterion was ≥9 Brix percent and was measured (data not shown) with an optical Brix refractometer (Master-T, Atago, Saitama, Japan). Fruits (125 g) were aseptically packed in polyethylene terephthalate containers (Nespak, Massa Lombarda, Italy) with a lid and holes for air circulation. Fruit samples were immediately transferred to the laboratory under cold conditions (3 ± 2 °C and 80–85% RH). Moldy and/or damaged fruits were discarded before analysis. Each of the packages was tested for NoV-RNA using the ISO 15216-2:2019 method

as described below before starting the experiments. The various experimental treatments were started approximately 8 h after harvest.

2.2. Viruses and cells

The murine norovirus 1 (MNV-1) was obtained from ATCC (# VR-1937) and propagated in RAW 264.7 (ATCC # TIB-71) mouse macrophage cells (Gonzalez-Hernandez, Bragazzi Cunha, & Wobus, 2012). The RAW 264.7 cells were maintained at 37 °C and 5% CO_2 in RPMI 1640 Medium (Millipore Sigma, Darmstadt, Germany) supplemented with 10% heat-inactivated FBS, 1% L-glutamine, penicillin (100 units/mL) and streptomycin (100 μg/mL). MNV-1 was propagated by infecting flasks of confluent RAW 264.7 cells with virus suspension with a multiplicity of infection (MOI) of 1 and incubation for 60 min at 37 °C and 5% CO_2 with gentle rocking. RPMI 1640 (15 mL) was then added to each flask and incubated for a further 24 to 48 h until cell lysis. Media and debris were collected and centrifuged at 500 ×*g* for 5 min at 4 °C. The supernatant was collected and the virus titer was determined by plaque-forming assay.

Hepatitis A virus strain HM175/18f was obtained from ATCC (# VR-1402) and propagated in fetal rhesus monkey kidney cells (FRhK-4, ATCC # CRL-1688). FRhK-4 cells were grown, and maintained and viral stocks prepared as described previously (Gosert, Egger, & Bienz, 2000). HAV titer was also determined by plaque-forming assay.

2.3. Plaque assay

MNV and HAV titers were quantified by plaque assay in 12-well plates (CLS3513, Corning, New York, USA). For quantification, the cell lines RAW 264.7 and FRhK-4 were infected with the stock virus supernatant or virus suspension eluted from contaminated berries. The cell monolayers were grown at 37 °C overnight, and each of the three wells was inoculated with 100 μL aliquots of the sample dilutions from virus suspension eluted from stock, control, and experimental group of raspberries. Virus suspensions were diluted using RPMI 1640, and were adsorbed for 60 min at 37 °C. To prevent cells from drying out, plates were gently tilted back and forth by hand every 15 min. Following incubation, the virus inoculum was removed from the plates, and cells were covered with 2 mL/well of a 1.6% carboxymethylcellulose overlay medium (Millipore Sigma # 419273). Plates were incubated at 37 °C with 5% CO_2 for 2 days (MNV) and 7 days (HAV). After incubation, the overlay medium was aspirated, cells were gently washed twice with phosphate-buffered saline (PBS; Capricorn Scientific, Ebsdorfergrund Germany, # PBS-1A) and monolayers were fixed with 10% buffered formalin (Millipore Sigma # HT501128-4 L) for a 2 h. The fixative was subsequently aspirated and discarded, and 200 μL of 0.5% crystal violet were added to each well and incubated at room temperature for 15 min. Plaques were enumerated and used for the calculation of virus titers in plaque-forming units per mL (PFU/mL).

2.4. Artificial contamination of raspberries

A 1-jet Collison nebulizer (BGI, Waltham, USA) was used for aerosol contamination of raspberries with MNV and HAV. An aliquot of 20 mL of each virus suspension was placed in the nebulizer. The concentrations of MNV and HAV in the aliquots were 2×10^9 PFU/mL and 4×10^{10} PFU/mL, respectively. The nebulizer flow rate was set at 2.0 l/min and 1380 hPa using nitrogen gas (N_2). Sample contamination by MNV and HAV was performed during a separate time interval. In order to obtain a sufficient volume of eluted virus for the evaluation of antiviral efficiency (PMA/RT-qPCR, TEM imaging, and infectivity assay) twenty-five-gram raspberry sample duplicates were contaminated with approximately 100 μL of respective virus aerosolized suspension for each experimental group. Samples were allowed to dry for 30 min in a biosafety cabinet and then stored at 4 °C in a refrigerator until treated with cold atmospheric plasma.

2.5. Cold atmospheric plasma treatment

The schematic of the pulsed positive corona discharge system for cold plasma virus inactivation is shown in Fig. 1. A lab-scale plasma power generator consisted of a low DC (12 V) to high voltage AC inverter (7 kV, 10 mA, MINIMAX70, Amherst, USA) coupled with 4-stage Cockcroft-Walton voltage multiplier. Each stage consisted of two high voltage capacitors (1 nF, 20 kV, Ceramic Disk Capacitor) and two diodes (25 kV, 5 mA, VG25/20 High Voltage Rectifier) and a discharge limiting resistor was set at the output. When operated at full output, the plasma generator was capable of delivering 50 kV DC at 0.5 mA in sub-microsecond high voltage pulses.

For cold plasma generation, two discharge electrode assemblies were employed. The high voltage electrode (anode) was made of the pure copper square bar which was cut into an array of triangular spikes using a waterjet cutter. Anode has been covered with epoxy resin acting as an electric insulator leaving pin-shaped spike ends free. The counter-electrode (cathode at ground potential) was made of copper-plated (18 μm thick) single-sided epoxy resin reinforced with fiberglass (thickness 0.6 mm). Both electrodes were placed in a 3 L food container box (Curver, USA) made of polypropylene and the anode was glued to the lid while the cathode was fixed below the anode (Fig. 1) so that the inter-electrode gap was 15 mm. For each treatment, a 2 × 25 g contaminated raspberry sample was carefully distributed at the bottom surface of the container. Cold plasma was generated by a positive corona discharge between the electrodes in the presence of synthetic air 5.5 (N_2 + O_2 20%; purity ≥99.9995%; H_2O < 2 ppm, CO + CO_2 < 0.1 ppm) (Messer, Serbia) introduced through the barb inlet with a gas fixed flow rate of 2.4 L/min. A SmartTrak 100 mass-flow controller (Sierra Instruments, Monterey, USA) was used to monitor the volume of working gas flowing through the system, in standard liters per minute. A small inline pressure regulator (Jain, USA) was attached to the container outlet to maintain plasma gas pressure within the container.

Treatments were carried out in the range of 0–10 min (0, 1, 3, 5, 7, and 10 min) at a 25 W power level. An exposure time of 0 min represented the control samples for each working session. The discharge power was calculated from total current and voltages curves measured at the output of the power generator, using a P6015A voltage probe (Tektronix, Beaverton, USA), a TCP312A (Tektronix, Beaverton, USA) current probe and an oscilloscope (Tektronix DPO2024B). A K-type thermocouple probe (Testo 926, Testo, Titisee-Neustadt, Germany) was introduced into the pressure regulator housing and used to measure the plasma temperature inside the food container box during the treatment. In all experiments, artificially contaminated samples without exposure to cold plasma were used as control samples.

In order to identify and measure the species produced by the pulsed corona discharge (RONS, in particular, O_3 and NO_x) causing virus inactivation, the discharge effluent was directed to gas analyzers at the location of the fruit samples. Gas composition was measured at 1-min, 3-min, and 5-min time points. For nitric oxide and nitrogen dioxide we utilized a Thermo Scientific 42iQ NO-NO_2-NO_x analyzer (Thermo Fisher Scientific, Waltham, USA) with a measuring principle based on chemiluminescence, and for ozone 106-MH Ozone Monitor (2B Technologies, Boulder, USA) based on single beam UV absorption at 254 nm.

2.6. Virus elution

The protocol included in the ISO 15216-1 (ISO, 2017) was used with slight modifications. Briefly, 25 g of raspberries were placed in a 400 mL Stomacher bag with a filter compartment. All samples were incubated at room temperature for 10 min. Thereafter, 40 mL of Tris-Glycine Beef Extract (TGBE)-Buffer (pH 8.5) and 30 units of pectinase (*A. niger*) (Millipore Sigma, Darmstadt, Germany) were added. The sample was incubated on a horizontal shaker for 10 min at room temperature (RT) with tilting. This step was followed by checking the pH value and readjusting to 8.5 with NaOH, when necessary. The pH value was

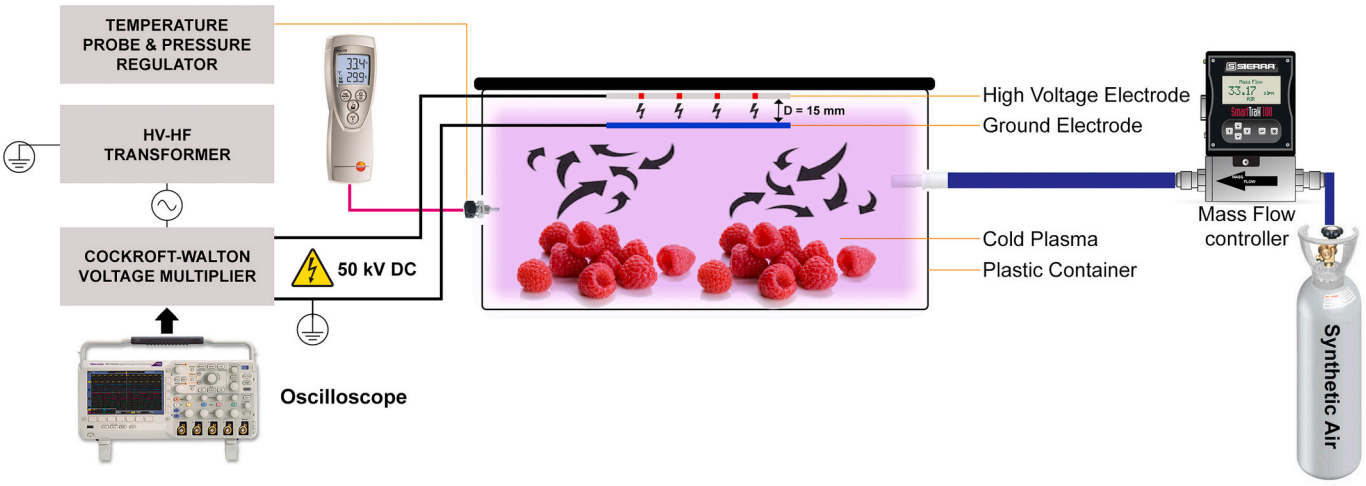

Fig. 1. Schematic of the plasma source and reactor setup used for inactivation of viruses on raspberries.

intentionally maintained at 8.5 to prevent overestimation of cold plasma efficiency as high alkaline pH may trigger alterations in capsid structure and possible denaturation of viral RNA. Next, the buffer solution was transferred to a 50 mL tube after passing through the stomacher bag's filter compartment. The solution was centrifuged at 4 °C and 10,000 ×*g* for 10 min to remove fruit debris. The cleared solution was transferred into a new tube, and the pH was adjusted to 7.0–7.2 with 1 N HCl and 10 mL of 5 × PEG/NaCl solution (500 g/L PEG 8000 (Millipore Sigma), 1.5 mol/L NaCl) was added. The mixture was shaken vigorously for 30 s and incubated for 1 h in a rotatory shaker at 4 °C and 70 rpm. This step was followed by centrifugation at 10,000 ×*g* and 4 °C for 30 min. The PEG formed a pellet and the supernatant was discarded. Another centrifugation at 10,000 ×*g* and 4 °C for 5 min was performed to compact the PEG pellet followed by the removal of liquid residues by pipetting. The pellet was dissolved in 500 μL PBS by vortexing and repeated pipetting. The solution was then transferred into a fresh Eppendorf tube and 500 μL of a chloroform/butanol mixture (1:1, *v*/v) was added. After vortexing and incubation for 5 min at RT, the sample was centrifuged at 10,000 ×*g* and 4 °C for 15 min. Thereafter, the upper aqueous phase (450–500 μL) was transferred to a fresh tube by pipetting. Samples were stored at −80 °C until used for TEM imaging, virus infectivity assay, and PMA/RT-qPCR.

2.7. Propidium monoazide treatment

The conventional RT-qPCR method amplifies total viral RNA found in a sample and cannot differentiate infectious and non-infectious MNV and HAV virions. Inability to distinguish infectivity status could result in falsely overestimating the number of viral genome copies in a sample and in turn underestimate the efficacy of CAP treatment. Thus, in addition to RT-qPCR, we utilized nucleic acid intercalating dye-coupled RT-qPCR to quantify the number of intact virus genome copies for each sample. From each experimental group, eluted virus samples were subjected to propidium monoazide (PMA) treatment. PMA is a dye that penetrates only damaged or structurally altered viral capsids and intercalates via covalent interactions into a viral genome after exposure to strong visible light and arrests the qPCR amplification. This approach effectively ensures that any signal detected in RT-qPCR would presumably originate from an infectious virus particle where the capsid still remains intact post cold plasma treatment.

PMA (Biotium, Hayward, USA) was reconstituted with 20% dimethyl sulphoxide (DMSO; Millipore Sigma, Darmstadt, Germany) to a concentration of 1 mg/mL (1.95 mM) and stored at −20 °C. In a dark room, 100 μL of stock PMA was added to 400 μL of eluted virus samples in a 1.5 mL Eppendorf tube. The final concentration of PMA was adjusted to 200 μM by adding nuclease-free water. Samples were mixed by vortexing and incubated at room temperature for 10 min. After incubation, the tubes were exposed to a beam of light generated by a 50 W Blue 460–470 nm LED COB module (Cree, Durham, USA) at a distance of 10 cm at room temperature for 20 min to photoactivate dye.

2.8. RNA extraction

Viral RNA was extracted with NucliSENS miniMAG (bioMérieux, Marcy l'Etoile, France) according to the manufacturer's instructions. The starting sample volume was approximately 400 and 500 μL and the elution volume was 80 μL. A negative extraction control with PBS was included in each extraction cycle. In order to reduce the influence of *co*-extracted RT-qPCR inhibitors such as polyphenols and/or anthocyanins, eluted RNA was purified using OneStep PCR Inhibitor Removal Kit (Zymo Research, Irvine, USA). Briefly, the Zymo-Spin III-HRC column cap was loosened, and 600 μL of Prep-Solution was added followed by centrifugation at 8000 ×*g* for 3 min. Next, the prepared column was transferred to a clean 1.5 mL microcentrifuge tube. An 80 μL sample of RNA was pipetted to the center of the resin in a column and centrifuged at 16,000 ×*g* for 3 min. After centrifugation, the purified RNA was present at the bottom of the tube. The purified RNA was directly used or stored at −80 °C until RT-qPCR analysis.

2.9. Construction of a DNA quantification standard for RT-qPCR

MNV DNA quantification standard was constructed as described by Kitajima et al., 2010. Briefly, a 500 bp fragment encoding the ORF1–ORF2 junction of the MNV-1 strain (accession No. DQ285629, 4887–5386 bp) was amplified by PCR with Platinum Taq DNA polymerase High Fidelity (Invitrogen, Carlsbad, USA). PCR products were cloned into a pEX-A2 vector (Eurofins Genomics, Ebersberg, Germany). For HAV quantification, a sequence corresponding to nucleotide 1–542 of the HAV genome (accession No. NC001489) was also ligated into a pEX-A2 vector (Eurofins Genomics) (Persson et al., 2021). Both plasmids were purified using a QIAprep Spin Miniprep Kit (Qiagen, Hilden, Germany) according to the manufacturer's instructions. Quantifications of both MNV and HAV plasmids were conducted using a Qubit 4.0 Fluorometer together with the appropriate kit (Qubit dsDNA HS kit, Thermo Fisher Scientific, Waltham, United States). The material was diluted to appropriate concentrations in 1× TE buffer (Millipore Sigma, Darmstadt, Germany), split into single-use aliquots, and stored at −70 °C.

2.10. RT-qPCR

One-step RT-qPCR was performed with the RNA UltraSense One-Step Quantitative RT-PCR System (Thermo Fisher Scientific, Waltham, USA) on an AriaMx Real-Time PCR System (Agilent Technologies, Santa Clara, USA). For both MNV and HAV, each reaction contained 500 nM forward primer, 900 nM reverse primer, and 150 nM probe (Table 1). For each sample, a total of 25 μL reaction mix was prepared with 20 μL of reagents and 5.0 μL of the sample. RT-qPCR was performed with RT at 55 °C for 1 h, inactivation of the reverse transcriptase and activation of the DNA polymerase at 95 °C for 5 min, 45 cycles of denaturation at 95 °C for 15 s, annealing at 60 °C for 1 min, and elongation at 65 °C for 1 min.

Quantification was performed using a ten-fold dilution series of each plasmid DNA. The calibration curve ranged from 1×10^8 to 1×10^1 genome copies per microliter of PCR (gc/μL) reaction. Results were analyzed with the Agilent Aria software, version 1.8.

2.11. Transmission electron microscopy

To analyze the ultrastructural changes in viruses subject to cold plasma treatment, transmission electron microscopy (TEM) was used. The carbon-coated grids (Agar Scientific, Stansted, UK) were placed onto a 20 μL drop of the virus eluate for 2 min. Afterward, grids were removed and the excess fluid was blotted by gently pushing the loop sideways on filter paper, the sample was then fixed in 2.5% glutaraldehyde in the same manner, air dried, stained with 2% uranyl acetate, and examined by a transmission electron microscope (Philips CM12, FEI Electron Optics, Eindhoven, The Netherlands) at 80 kV equipped with the SIS MegaView III camera (Olympus Soft Imaging Solutions, Münster, Germany). Acquired TEM images were used for virion ultrastructure and size analysis by employing the iTEM software (Olympus Soft Imaging Solutions, Münster, Germany).

2.12. Instrumental measurement of color

The surface color of control and cold plasma-treated raspberries was analyzed using a CR400 Chroma Meter colorimeter in reflectance mode (Konica-Minolta, Japan) according to the manufacturer's instructions. The 10° standard observer adjustment (10° dihedral angle) was chosen. Illuminant D65 was used (daylight source), following the CIE Lab recommendations. A 30 mm target mask was used. For calibration, a white (Y-87.2, x-0.3173, y-0.3348) and black reference standard tile was used. A glass sample measuring cup was filled to top with raspberries for color measurement. The color was evaluated using the L*, a*, and b* values.

Table 1
Oligonucleotides for TaqMan-based MNV and HAV RT-qPCR used in this study.

Name	Sequence (5′ - 3′)[a]	Position	Reference
MNV-f	CCG CAG GAA CGC TCA GCA G	5028-5046[b]	Kitajima et al. (2010)
MNV-r	GGY TGA ATG GGG ACG GCC TG	5156-5137[b]	Kitajima et al. (2010)
MNV-probe	FAM - ATG AGT GAT GGC GCA - BHQ1	5062-5076[b]	Kitajima et al. (2010)
HAV-f	CTC TTT GAT CTT CCA CAA GRG GT	373-395[c]	Persson et al. (2021)
HAV-r	GCC GCT GTT ACC CTA TCC AA	444-463[c]	(Jiang et al., 2014; Persson et al., 2019; Win et al., 2019)
HAV-probe	FAM - AGG CTA CGG GTG AAA C - BHQ1	396-411[c]	Persson et al. (2021)

FAM = 6 carboxyfluorescein, BHQ1 = Black Hole Quencher.
[a] Mixed bases in degenerate primers and probes are as follows: Y ≈ C or T; R ≈ A or G.
[b] Corresponding nucleotide position of Murine norovirus 1 strain SC/2014/USA (accession number: KM102450.1) as reference.
[c] Corresponding nucleotide position of Hepatitis A virus strain HM175/18f (accession number: M59808) as reference.

In order to describe the overall difference between the colors of the non-treated and CAP-treated raspberries, the mean values of L*, a*, and b* were determined to calculate the ΔE*ab value (Kuehni, 1976). Each sample was analyzed in 6 replicates for a robust assessment of color variability.

2.13. Modelling of inactivation kinetics and statistical analysis

Two different inactivation models were compared to appropriately describe the inactivation kinetics: the biphasic and the Weibull model, respectively. Regression analysis of viral inactivation data was performed using the GInaFiT software (Geeraerd, Valdramidis, & Van Impe, 2005). The regression coefficients (R^2) and root mean square error (RMSE) values were used to evaluate model fitness. The time required to obtain 4 $\log_{10}$ reduction was calculated for each model. The confidence level used to determine statistical significance was 95%.

All experiments were carried out in triplicate, and results are presented as the mean and standard deviation, and they were considered statistically significantly different at $p \leq 0.05$. Results were subjected to a one-way analysis of variance (ANOVA) using Minitab 17 Statistical Software (Minitab LLC, State College, USA). Post hoc ANOVA Tukey's multiple range test was used to compare the differences in mean values between treatment groups over time while paired *t*-test was used to compare the differences in mean values between non-PMA- and PMA-treated samples.

3. Results

3.1. Plasma gas temperature during the CAP treatment

Plasma generated in the PCDP setup emits low-temperature plasma gas in the surrounding air. Since plasma gas can keep temperatures below 42 °C, it can come in touch with the soft matter without causing thermal damage. In consideration of the structural sensitivity of raspberries at high temperatures, we measured plasma gas temperatures at different time intervals during the CAP treatment (Fig. 2). Plasma gas temperatures were also measured to ensure the treatment in itself did not produce a thermal inactivation effect on MNV and HAV and lead to overestimation of CAP efficiency.

The graph of temperature as a function of PCDP exposure time indicates that the gas temperature increased continuously by increasing the operation time, at an average rate of 1.9 °C per minute. At 0 min, the plasma temperature inside the container was 22.4 ± 0.8 °C. Even after 10 min, the gas temperature was as low as 41.4 ± 1.3 °C.

3.2. O_3, NO, and NO_2 concentration in PCDP plasma

Concentrations of ozone, nitric oxide, and nitrogen dioxide as the major reactive species in PCDP plasma were measured inside the plasma reactor at different time points (Table 2). Ozone was the most abundant reactive species and maintained a high level of production throughout the CAP treatment period. On the contrary, the concentration of nitric oxide was below the limit of detection, while the concentration of nitrogen dioxide became detectable after 3 min and slowly raised at 5-min time point.

3.3. Efficacy of CAP treatment based on RT-qPCR analysis

The raspberries inoculated with MNV and HAV, respectively, were treated with cold plasma generated by PCDP setup for 1, 3, 5, 7, and 10 min to assess the antiviral activity of the CAP treatment against the two viruses on berry fruit. In the control group of raspberries (no CAP treatment) the mean initial MNV titer recovered was 5.76 $\log_{10}$ gc/μL while the HAV titer was 6.47 $\log_{10}$ gc/μL. Results of MNV and HAV inactivation on raspberries (quantified using both RT-qPCR and PMA-RT-qPCR) following a 1, 3, 5, 7, and 10-min exposure to cold plasma

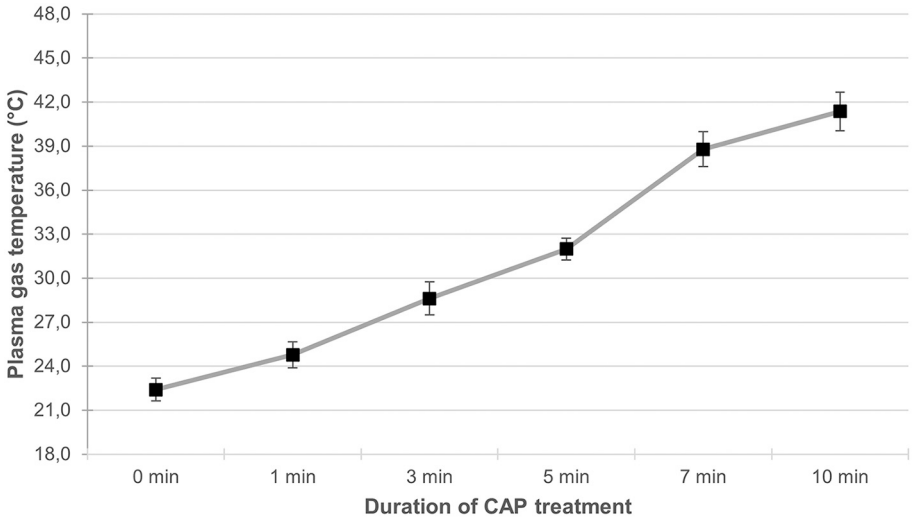

Fig. 2. Graph of temperature as a function of plasma exposure time. The data represent the mean of three replicates. The error bars represent standard deviation.

Table 2
Ozone, nitrogen dioxide, and nitric oxide concentration during CAP treatment.

Duration of cold plasma treatment	O_3 (ppm)	NO_2 (ppm)	NO (ppm)
1 min	875	< 1	0
3 min	1850	14	0
5 min	1725	223	0

are shown in Fig. 3.

3.4. Influence of CAP treatment on virus infectivity

The infectivity reduction of MNV and HAV recovered from CAP-treated raspberries over a 10-min interval exposure time is shown in Fig. 4. Cold plasma treatment contributed to progressive loss of infectivity for both viruses, resulting in >4 $\log_{10}$ (≥ 99.99%) reduction. However, the kinetics of MNV infectivity reduction compared to HAV was significantly different. For MNV, infectivity reductions of 0.74, 2.24, 4.22, 4.69, and 4.81 $\log_{10}$ PFU were observed after 1, 3, 5, 7, and 10 min, respectively. Similarly, HAV infectivity reductions of 0.55, 2.12, 3.09, 3.51, and 4.09 $\log_{10}$ PFU were observed after the same time intervals. Results suggested that CAP treatment was more effective against MNV vs. HAV with a higher infectivity reduction (4.22 vs. 3.09 $\log_{10}$ PFU) achieved in a shorter exposure time (5 vs. 10 min).

3.5. Structural deformation of viral capsid upon CAP treatment

Transmission electron microscopy was performed to provide evidence of plausible MNV and HAV capsid deformation following CAP treatment at different time intervals. As shown in Table 3, at 0-min outer diameter of MNV was approximately 29 nm, and by increasing exposure time MNV capsid size increased almost exponentially ($p \leq 0.05$) reaching a peak after a 5-min treatment (outside diameter was 128 nm). Interestingly, after 7-min, the diameter decreased to just 38 nm and after 10-min, the size of the remaining virions reduced further to approximately 17 nm. A similar trend was observed in impact on HAV capsid size, at 0-min the outer diameter was approximately 27 nm and by increasing exposure time HAV capsid size increased ($p \leq 0.05$) reaching a peak between 3- and 5- min of treatment, to approximately 70 nm. Again, at 7-min treatment, the diameter decreased to 50 nm by 10-min, and the size of remaining virions reduced to approximately 21 nm. Both MNV and HAV demonstrated viral capsid diameter kinetics that closely resembles a parabolic curve throughout the ten-minute CAP treatment.

In comparing the MNV and HAV virion diameters at their peak (5-min treatment point) there was a significant statistical difference in their maximum size, indicating that the MNV capsid structure was less resistant to cold plasma treatment compared to the HAV capsid. TEM images for MNV (Fig. 5) taken at respective CAP treatment time intervals further confirmed dramatic ultrastructural changes

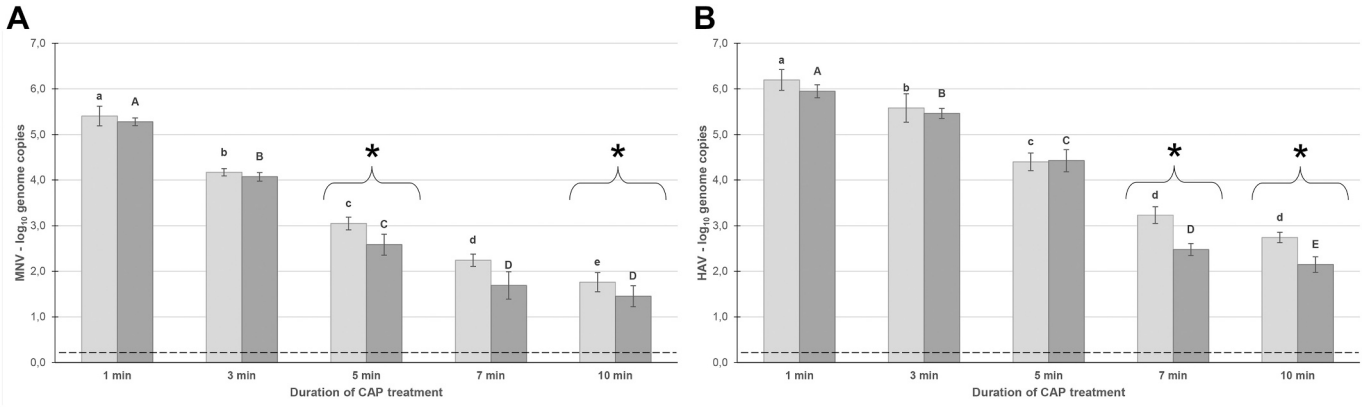

Fig. 3. The impact of cold plasma treatment on the inactivation of MNV (A) and HAV (B) on raspberries followed by RT-qPCR. Dark and light grey shaded bars represent $\log_{10}$ genome copies in samples with and without propidium monoazide (PMA) treatment. The data represent the mean of three replicates. The error bars represent standard deviation. Means with different superscript letters differ significantly ($p \leq 0.05$). Asterisks (*) also indicate a significant difference ($p \leq 0.05$) between non-PMA and PMA-treated samples by paired *t*-test. The dashed lines indicate LOD of the RT-qPCR assay.

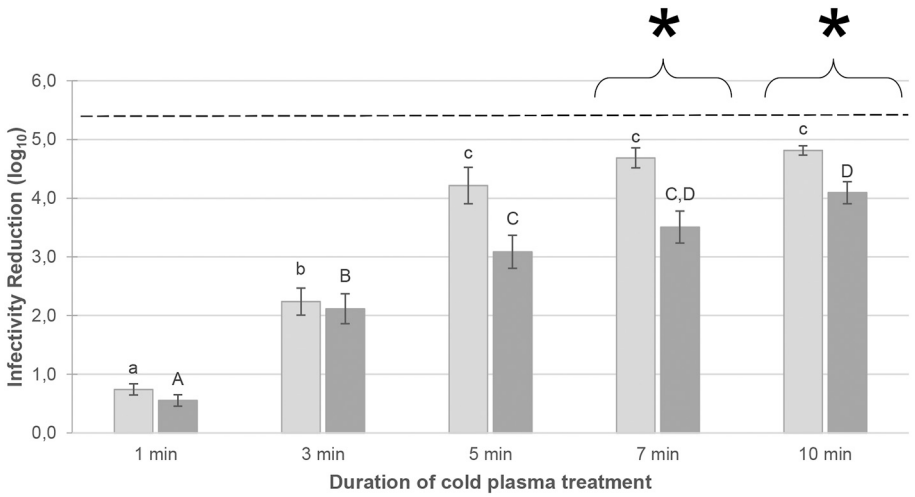

Fig. 4. The impact of cold plasma treatment on the reduction of viral infectivity for a MNV (light grey bar) and HAV (dark grey bar) compared to the untreated control. The data represent the mean of three replicates. The error bars represent standard deviation. Means that do not share a letter are significantly different ($p \leq 0.05$).

Table 3
Changes in virion size (nm) during the CAP treatment.

Duration of cold plasma treatment	MNV	HAV
0 min	28.80 ± 1.61^{a}	27.21 ± 0.29^{a}
1 min	58.53 ± 2.47^{b}	33.78 ± 1.92^{b}
3 min	86.30 ± 7.02^{c}	68.07 ± 3.08^{c}
5 min	127.99 ± 10.18^{d}	71.75 ± 1.58^{c}
7 min	$37.77 \pm 5.94^{a,e}$	50.60 ± 0.91^{d}
10 min	17.37 ± 1.34^{e}	21.72 ± 1.47^{e}

All the data are expressed as mean of three replicates ± standard deviations. Means that do not share a letter are significantly different ($p \leq 0.05$).

demonstrated as an initial increase of MNV virion particle sizes (1- and 3-min treatment), followed by critical swelling and disintegration of capsomers (5-min treatment) and succeeded by loss of surface proteins and forming "bald" surfaces causing coalescence of virions into larger ring-like structures (7-min treatment) resulting in the discharge of material from virion central core and collapse of capsid coat remnants (10-min treatment).

3.6. Modelling CAP antiviral kinetics

To properly describe MNV and HAV survival curve kinetics following CAP treatment we have tested two different models, i.e., the biphasic and Weibull frequency distribution model. Goodness-of-fit indicators for both models are shown in Table 4 and respective inactivation curves are shown in Fig. 6.

The biphasic virus inactivation model showed a better fit of the experimental data for MNV compared to the Weibull model having significantly higher R^2 (0.99 vs. 0.85) and a lower RMSE (0.14 vs. 0.84). The same is true for HAV where analysis of kinetics data showed R^2 values to be higher (0.99 vs. 0.93) and RMSE values to be lower (0.10 vs. 0.41) in the biphasic model. It was observed that for 4 log_{10} reduction of MNV, a 25 W CAP treatment time of 4.7 min is required. In contrast, HAV required a treatment time of 9.8 min for a 99.99% reduction.

3.7. Effect of CAP treatment on raspberry color parameters

To assess any potential color changes caused by the exposure to cold plasma, the CIE Lab L* (light vs. dark), a* (red vs. green), and b* (yellow vs. blue) values of raspberries were measured before and after treatment (Table 5). The average values of L*, a*, and b* for raspberries before treatment were observed as 31.61 ± 1.35, 24.88 ± 0.58, and 8.72 ± 0.79, respectively. Overall, no significant ($p > 0.05$) changes in L*, a*, b* in samples were observed during the 7-min CAP treatment. At that point, a significant ($p \leq 0.05$) decrease in L* color parameter (28.03 ± 0.97) was observed with further reduction noted at 10-min treatment ($p \leq 0.05$).

As for the a* and b* values, no statistically significant ($p > 0.05$) changes were observed in the first 7 min of CAP treatment, however

Table 4
Goodness of fit and model parameters.

Virus	Model	R^2	RMSE	4D time
MNV	Biphasic	0.99	0.14	4.7 min
	Weibull	0.85	0.84	7.4 min
HAV	Biphasic	0.99	0.10	9.8 min
	Weibull	0.93	0.42	9.5 min

R^2 – regression coefficient; RMSE - Root mean square error; 4D time - the time required for a 4 log_{10} reduction.

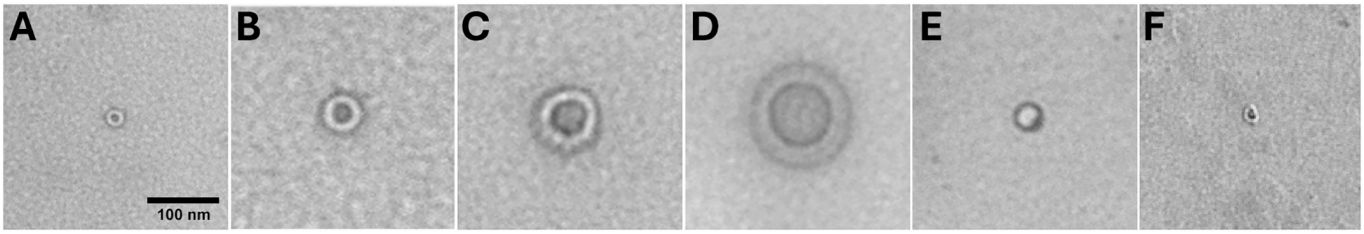

Fig. 5. The impact of cold plasma treatment on the MNV capsid structure by transmission electron microscopy (magnification 40,000 ×). Images were taken at respective CAP time intervals: 0 min (A), 1 min (B), 3 min (C), 5 min (D), 7 min (E) and 10 min (F).

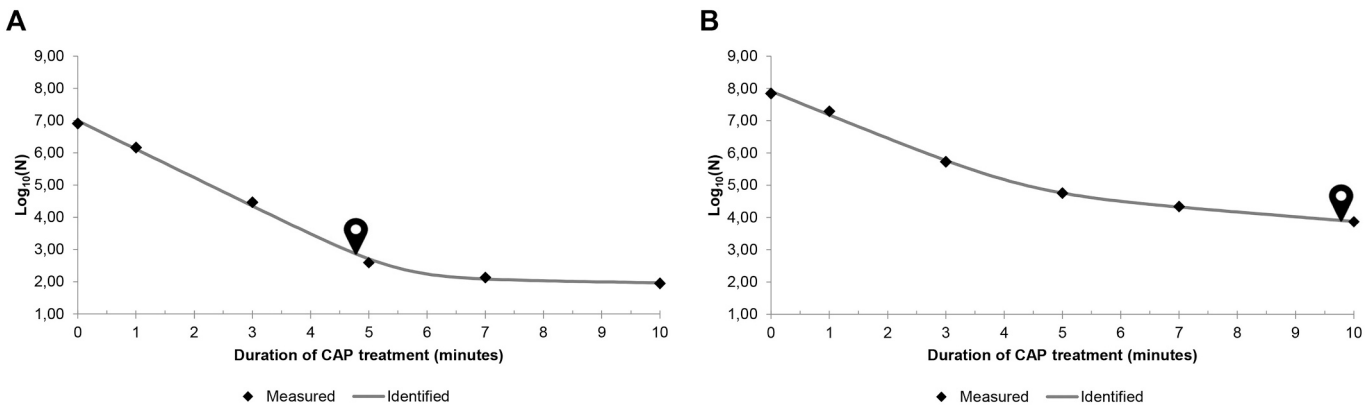

Fig. 6. Survival curves of MNV (A) and HAV (B) in raspberries treated with CAP, biphasic model.

Table 5
Effect of cold plasma treatment on raspberry color parameters.

Duration of cold plasma treatment	L*	a*	b*	ΔE*
0 min	31.61 ± 1.35[a]	24.88 ± 0.58[a]	8.72 ± 0.79[a]	
1 min	32.70 ± 0.89[a]	24.82 ± 1.38[a]	8.28 ± 1.02[a]	1.18
3 min	31.08 ± 1.09[a]	24.95 ± 0.57[a]	8.34 ± 0.84[a]	0.66
5 min	31.91 ± 1.04[a]	25.28 ± 0.82[a]	8.30 ± 1.15[a]	0.65
7 min	28.03 ± 0.97[b]	23.96 ± 0.71[a]	8.98 ± 0.68[a]	3.71
10 min	25.72 ± 0.61[c]	21.49 ± 1.29[b]	10.73 ± 0.62[b]	7.09

All the data are expressed as mean of three replicates ± standard deviations. Means that do not share a letter are significantly different ($p \leq 0.05$).

significant decrease (21.49 ± 1.29) and increase (10.73 ± 0.62)), were observed at the 10 min point for a* and b* values, respectively. These results implicated that the treatment with cold plasma at the power rate of 25 W showed negligible color changes in the first 7 min of exposure, but in the interval from 7 to 10 min color changes are notably apparent in comparison to untreated raspberries.

4. Discussion

Outbreaks attributed to consumption of non-thermally treated foods contaminated with foodborne enteric viruses have not abated and continue to be a global public health concern. A variety of mitigation measures including improved water treatment and quality testing, personal hygiene, and waste management are commonly applied, however, a reliable non-thermal intervention that can effectively reduce the risk is not availed by growers and processors in the industry. Cold atmospheric plasma has recently gained attention as a potential antiviral tool that could overcome limitations of the existing food safety control measures in heat-sensitive products (Aboubakr et al., 2020; Ahmed, Maunula, & Korhonen, 2020; Bunz et al., 2018; Choi et al., 2020a; Fuentes et al., 2021). The main benefits of CAP are prevention of post-harvest contamination, non-toxicity, and reduction of potentially hazardous chemical agents, which is also beneficial from an environmental standpoint (Filipić, Gutierrez-Aguirre, Primc, Mozetič, & Dobnik, 2020; Weiss et al., 2017).

This was a unique study that investigated the inactivation of HuNoV viral surrogate (MNV) and HAV on contaminated raspberries by CAP in form of pulsed corona discharge plasma. So far, there have been just four studies published on the similar topic (Ahmed et al., 2020), but these dealt with assessment of the potential of CAP for treatment of contaminated lettuce (Aboubakr et al., 2020), turkey deli meat (Bozkurt, D'Souza, & Davidson, 2015b) and blueberries (Lacombe et al., 2015; Lacombe et al., 2017). Overall, the results from this study indicate that CAP could be used as an efficient decontamination tool in production and processing of raspberries. Previous research studies on inactivation of viruses (Alekseev, Donovan, Limonnik, & Azizkhan-Clifford, 2014; O'Connor, Cahill, Daniels, Galvin, & Humphreys, 2014; Pradeep & Chulkyoon, 2016; Choi et al., 2020a) employed conventional DBD plasma setup, which is of limited practical use due to a confined plasma production space which reduces the volume of treated fruit. In contrast, PCDP setup enables unrestricted propagation and circulation of low temperature plasma within the reactor vessel thus exposing large volume of viral contaminated fruit to reactive oxygen species (ROS), reactive nitrogen species (RNS), and other charged particles.

Since raspberries require use of ambient temperature processes for ensuring safety without compromising product quality, maintenance of low temperature cold plasma has been of utmost importance. In our experiment maximum antiviral effect was accomplished in 5–7 min treatment time (at 25 W) where plasma temperatures ranged from 33 to 39 °C. Obtained results were somewhat similar with those observed by Lacombe et al. (2015). In their research study, plasma temperature raised steadily from room temperature until reaching 46 °C after 2 min, i.e., temperatures >38 °C were observed after 30 s and remained steady. The same author (Lacombe et al., 2017) subjected blueberries inoculated with TV and MNV-1 to a CAP jet for 0 to 120 s. Product temperatures increased to 70 °C when treatment durations were 60 s. To mitigate the thermal effect, an air stream at ambient temperature was channeled onto the berries during treatment, limiting the rise in berry temperatures to approximately 47 °C by the end of the 2-min treatment. However, in the study conducted by Starek et al. (2020) aimed to extend the shelf life of tomato juice, the temperature of the juice increased only slightly to a maximum of 29 °C, even after the longest CAP treatment (10 min). Similar trend was confirmed by Capelli et al. (2021) who used cold plasma sanitation system to inactivate SARS-CoV-2 RNA on packaged foods and maximum measured plasma gas temperature was below 34 °C. Different plasma temperatures could surely be explained by different setups of CAP reactor, feeding gas composition and flow rate as well as variable degree of ionization. We have demonstrated that plasma temperature was too low to induce unfavorable quality changes in raspberries, and was considerably lower than reported temperatures required for inactivation of foodborne viruses (T_i), i.e., $FCV_{Ti} = 63.3$ °C, $NoV_{Ti} = 76.6$ °C and $HAV_{Ti} = 85.0$ °C (Bidawid, Farber, Sattar, & Hayward, 2000; Topping et al., 2009). In the view of the findings in our study, we can assert that the CAP treatment in PDCP setup was verified to be nonthermal in nature and its temperature does not contribute to the MNV and HAV inactivation for the conditions of this study.

The analysis of the gas phase compounds of a cold atmospheric plasma is of an essential importance for a comprehensive understanding

of the effects it can induce on target viruses (Simoncelli et al., 2019). Air plasma chemistry has been extensively studied for many years due to increased use of commercial ozonizers and it is well known that ozone is dominantly generated at relatively low power (sometimes called a 'silent discharge') in air DBD and corona discharges that form around high voltage surfaces with sharp points or small radii of curvature (Moldgy, Nayak, Aboubakr, Goyal, & Bruggeman, 2020). However, unlike classical ozonizers, DBD and corona discharges exhibit unique transition in production of reactive species once the input power exceeds certain critical value which reflects as increase of nitric oxide and nitrogen dioxide leading to gradual ozone quenching ("discharge poisoning"). An excellent studies performed by Shimizu, Sakiyama, Graves, Zimmermann, and Morfill (2012) and Simoncelli et al. (2019) demonstrated that critical power level which triggers transition from "ozone mode" to "RNS mode" is 0.1 W/cm^2. In our study ozone was the most abundant reactive species, exponentially raising to 850 ppm in 60 s and maintained a high concentration (above 1500 ppm) throughout the CAP treatment period. This was in accordance with results obtained by Capelli et al. (2021) who employed surface DBD plasma device to decontaminate food packaging previously contaminated with SARS-CoV-2 RNA. In their study it took about 50–90 s (depending of volume) for O_3 to reach maximum concentration of 1700 ppm which remained stable until the end of experiment. Same pattern of ozone production was seen in a study by Shimizu et al. (2012).

When it comes to nitric oxide, this reactive species was not detected in our study. This is in agreement with findings of Shimizu et al. (2012), Mohamed et al. (2021) and Simoncelli et al. (2019). Namely, absence of nitric oxide has been anticipated after we found a significant amount of ozone in the corona's effluent. Indeed, in an ozone rich mixture NO quickly converts to NO_2 according to the following reaction: $NO + O_3 \rightarrow NO_2 + O_2$. As for the NO_2 traceable amount was detected in 3-min time point, while in 5-min timepoint its concentration increased to approximately 250 ppm. Gradual increase of NO_2 can be explained by prolonged CAP treatment time when keeping the plasma source without adjusting the input power, voltage, and frequency, ozone will be subsequently quenched and partially converted into various nitrogen oxides. This was in accordance with the results of study by Moldgy et al. (2020) who demonstrated that after 4 min of DBD plasma treatment concentrations of O_3 and NO_2 almost equalized in the "transient" mode (ozone ➔ NO_2) and further exhibited 4.5 $\log_{10}$ inactivation of FCV.

For evaluation of functional antiviral effectiveness of cold plasma, we employed two different approaches: measuring reduction of viral titers by RT-qPCR and determining reduction of virus infectivity by plaque assay. Each technique alone has its own drawbacks which could potentially underestimate employed antiviral strategy. Counting of viral RNA genome copies by RT-qPCR usually does not correlate with the number of infectious virions (Butot, Putallaz, & Sánchez, 2008; Randazzo, López-Gálvez, Allende, Aznar and Sánchez, 2016). Also, determination of virus infectivity by plaque assay can underestimate virus infectivity levels by at least 2 to 3 orders of magnitude (Hewitt, Leonard, Greening, & Lewis, 2011; Thebault, Teunis, Le Pendu, Le Guyader, & Denis, 2013). Current scientific opinion deems antiviral processes as efficient if reaching at least >3 $\log_{10}$ reduction of infectious viruses (Codex Alimentarius, 2012). However, we felt that for a CAP-mediated risk mitigation for contaminated berries a more stringent performance criterion (> 4 $\log_{10}$ reduction) should be considered as the uncertainty in the estimates can be substantial. To more accurately assess antiviral effectiveness using RT-qPCR, we used an additional molecular pretreatment using PMA RNA intercalating dye (Randazzo et al., 2018).

Results indicated that CAP treatment induced 4 $\log_{10}$ reduction in titer of both MNV and HAV viral genome copies in contaminated raspberries after approximately 7 min. Compared with RT-qPCR alone, PMA treatment allowed additional $\log_{10}$ reductions of 0.55 and 0.75, for MNV and HAV, respectively. Additive reduction by PMA was noticed at all treatment times for MNV. However, the 4 $\log_{10}$ infectivity reduction of MNV measured by plaque assay occurred after <5 min. This is consistent with results obtained by Aboubakr et al. (2020) where a reduction by just 2.6 $\log_{10}$ HuNoV genome copies after 5 min exposure to CAP was achieved with no significant difference ($p > 0.05$) between treatment on both stainless steel and lettuce samples. Also, changes of the FCV titer in the same study showed similar pattern to results we obtained with MNV, i.e., FCV infectivity was reduced by ≈ 3 $\log_{10}$ during 3-min treatment time, as measured by plaque assay but the same samples showed only ≈ 2 $\log_{10}$ reduction in FCV genome copy number when EMA-RT-qPCR titration was used. Superior norovirus virucidal effect obtained by positive pulsed corona discharge cold plasma setup in the present study was in contrast to reduction patterns reported by Ahlfeld et al. (2015) who reported a slow and gradual 1.69 genome copies/mL reduction in HuNoV GII.4, achieved by surface micro discharge plasma (8.5 kV, 1 kHz) for 15 min. This was also the case with the results of Bae, Park, Choe, and Ha (2015), who inoculated MNV into fresh meat and treated with glide arc-plasma-based jets for 20 min, resulting in a reduction of virus infectivity of approximately 2 $\log_{10}$ PFU/mL. Even slower virucidal effect was demonstrated in a recent study by Choi et al. (2020a) on the impact of the DBD plasma treatment on HuNoV viability in oysters, who showed that DBD plasma treatment for 60 min achieved negligible reduction in HuNoV genomic titer reduction (< 1 $\log_{10}$ copy number/μL). Alternatively, when PMA treatment was used, HuNoV titer was reduced to >1 $\log_{10}$ gc/μL in 30 min. In contrast, virucidal effect obtained in our study was inferior compared to results obtained by Lacombe et al. (2017), the maximum log reduction for Tulane virus (also surrogate) in CAP treatment of blueberries was attained significantly faster, i.e., 3.5 $\log_{10}$ PFU/g after 2 min of treatment, while MNV was significantly reduced by 0.5 $\log_{10}$ PFU/g compared to the control at 15 s. Further treatment of MNV with ambient air brought the reduction to >5 $\log_{10}$ PFU/g at 1.5 min of treatment in the study by Lacombe et al. (2017), which we could not achieve even after 10 min of CAP exposure.

Hepatitis A virus, a member of *Picornaviridae*, showed higher resistance toward CAP treatment. Although 4 $\log_{10}$ MNV viral titer loss was achieved in 7 min, it took almost 10 min for HAV to reduce infectivity of the same order of magnitude. In raspberries contaminated by HAV and treated by CAP for 7 and 10 min, the virus titer reduction level was higher when measured by PMA-RT-qPCR compared to reduction of infectivity measured by plaque assay i.e., no additive effect of PMA was noticed.

It is quite complex to explain variability of results obtained by different research groups since majority of studies have an apparent limitation reflected in usage of cultivable surrogate viruses (e.g., MNV, Tulane virus and FCV), that are genetically similar to human norovirus and possess a similar biochemical and/or biophysical properties (but which cannot be propagated easily in cell culture). Yet, due to subtle differences in amino-acid structure of viral capsids surrogates cannot mimic authentically HuNoV, which is more environmentally stable than its proxies (Bozkurt et al., 2015a). Additionally, plasma treatment for microbial reduction depends primarily on the plasma difference, such as type of plasma discharge, plasma exposure type, injected gas type, electrode configuration, and frequency of applied voltage (Weltmann et al., 2010). We speculate that superiority of our CAP plasma treatment versus DBD lays in the specific setup used. Namely, corona discharge propagates away from the high voltage electrodes and plasma expands into a region free from high voltage (Laroussi, 2020). Although such plasma does not cause direct electrical impairment to the viruses, plasma exhibit a very high sudden local electric field which results in production of vast amount of highly potent and reactive species upon discharge, in amounts that greatly exceed those generated in DBD plasma setup. Knowing that corona plasma discharges are emitted as discrete plasma bullets propagating at high velocities (Lu & Laroussi, 2006) we hypothesize that tremendous virucidal effect is accomplished by the ability of reactive species to permissively penetrate inter-capsid joints and damage viral RNA. Next, when the role of O_3 produced by cold plasma was assessed, it was observed that the virus inactivation was enhanced by the presence of RNS (Mohamed et al., 2021). Further

studies showed that the combination of O_3 and NO_2 in the gas phase leads to the production of N_2O_5, which most likely leads to the formation of peroxynitrite (ONOO−/ONOOH) in the humid water layer on the substrate being treated (Mohamed et al., 2021; Moldgy et al., 2020; Simoncelli et al., 2019).

Due to uncertainties in discrimination between infectious and noninfectious virions using PMA-RT-qPCR, we further validated CAP treatment effect on virus capsid integrity by TEM imaging of respective viruses eluted from treated raspberries at each treatment timepoint. TEM analysis demonstrated that control MNV and HAV virions seemed intact and of usual size (≈ 29 nm and ≈ 27 nm, respectively). During the CAP exposure we observed considerable deformation of viral capsids manifested by increasing outer diameters, initially to the account of increase of intra-capsid volume and within 5 min by thickening of capsomers themselves (Fig. 4). MNV reached a maximum of 4.4-fold diameter of the control in just 5 min of CAP exposure followed by capsid bursting and intra-capsid content discharge (7 min). MNV capsid was found distorted and collapsed having just 60% of its original size after 10 min. It is interesting that eluted HAV virions did not suffer such a dramatic structural degradation as MNV virions. The maximum recorded size was 2.50- and 2.63-fold larger than control HAV in period between 3 and 5 min of treatment, respectively, and by the end of CAP operation time capsid slowly "deflated" reaching 80% of control HAV size. These results were consistent with TEM findings observed by Aboubakr et al. (2018) who showed destruction of a majority of viral capsids in plasma exposed FCV. Our TEM imaging results were also in accordance with report of Wu et al. (2015) who presented electron microscopy showing strong capsid damage in bacteriophage MS2 (nonenveloped RNA virus) by CAP treatment. It is important to note, that the present TEM imaging cannot serve alone as evidence of absolute virucidal activity since not all MNV and HAV virions were damaged during the CAP treatment, indicating influence of other processes. For this reason, PMA-RT-qPCR and plaque assay should be used concomitantly with TEM or other independent techniques (e.g., SDS-PAGE or HGBA assay) to guarantee proper quantification of infectious and intact virions.

On the basis of magnitudes of titer and infectivity reduction, as well as magnitude of structural deformation we demonstrated that HAV virus is more resistant to CAP treatment compared to MNV (plausibly to HuNoV). This is consistent with results obtained in a study by Nasheri, Harlow, Chen, Corneau, and Bidawid (2021) who applied advanced oxidative processes (hydrogen peroxide vapors, ozone and UVC light) for reduction of FCV, MNV and HAV in chocolate, pistachio and cornflakes. Their study demonstrated that HAV inactivation in chocolate was <2 $\log_{10}$ during a 1 min exposure, unlike with MNV where inactivation reached 4 $\log_{10}$. The genome of HAV is clearly more resistant to degradation triggered by the oxidative treatments compared to FCV and MNV, as the RNA genome reduction never exceeded 0.65 $\log_{10}$, while at least 2 $\log_{10}$ reduction was observed for the genome of FCV and MNV in chocolate after treatment for 60 s. In their opinion, the reduction of HAV titer was lower than reduction of infectivity indicating that at least a portion of surviving genomes that are quantified by RT-qPCR did not represent infectious particles. Similar pattern of infectivity reduction during positive pulsed corona discharge plasma treatment was demonstrated in a study by Song et al. (2022). This study evaluated the inactivation efficacy of PCDP to viruses using spring viremia of carp virus (SVCV) as a model. The results showed that 4 $\log_{10}$ reduction of SVCV infectivity in cells was reached after 120 s treatment.

When it comes to the practical application of cold plasma in the berry industry, a predictive model of virus survival would be advantageous for processors to incorporate effective post-harvest raspberries decontamination measures. The inactivation of microorganisms using plasma treatment typically results in an exponential decay, depending on time (Choi et al., 2020b). In our study analysis of kinetics data showed that Weibull model was not a good fit for the experimental data obtained due to poor regression coefficients and root mean square error values used to evaluate model fitness (Table 4). In contrast, a biphasic model proposed by Cerf (1977) showed exceptionally better model fitness and we are of opinion that it could be used successfully to describe CAP inactivation of MNV and HAV in raspberries. Both viruses studied were susceptible to plasma treatment, but experimental inactivation data and predicted parameters showed that MNV was more sensitive to plasma treatment than HAV. Calculated 4D value for CAP reduction of MNV was 4.7 min at 25 W, while calculated 4D value for HAV was almost doubled in comparison i.e., 9.8 min. Our model was not consistent with Choi et al., 2020a since these researchers suggested that HuNoV GII.4 inactivation in commercial raw oysters using DBD plasma can be successfully modeled using first-order kinetics where D1 and D2 values were 36.5 min and 73.0 min, respectively. We speculate that differences in approaches to setup CAP generation (PCDP vs. surface DBD) reflect these variabilities.

Raspberries' color is major post-harvest quality parameter that directly affects consumer perception and overall sensory acceptability. In raspberries, visible red color is correlated with total anthocyanin content and it is low in yellow fruit mutants and very high in black raspberries (Anttonen & Karjalainen, 2005; Weber, Perkins-Veazie, Moore, & Howard, 2008). Characteristic raspberry color also depends on amount of epicuticular wax deposited on the surface of raspberry fruit (Griffiths et al., 2000). During the 7 min of treatment there were no significant changes in L*, a*, and b* parameters noticed. At that time point, slight but statistically significant decrease in L* value (lightness) was observed indicating darkening of samples. However, by the 10 min timepoint the raspberries color became statistically more dark (lower L*), with less redness (lower a*) and less yellowness (lower b*) in comparison to the control. The overall color changes (ΔE*) for raspberries treated with CAP during 7 min fell between 0.65 and 3.71, compared to the controls. Even though the color difference might be perceptible through close observation when ΔE* lies between 1.5 and 5, the difference in fruit color becomes evident at glance only when ΔE* is higher than 5 (Obón, Castellar, Alacid, & Fernández-López, 2009). This was noticed in raspberries treated with CAP for 10 min where ΔE* equaled to 7.09. Thus, under plasma-treatment conditions (1–7 min at 25 W) investigated in the present study, the color quality of the raspberries was not affected evidently.

Similar darkening of CAP treated blueberries was reported by Sarangapani, O'Toole, Cullen, and Bourke (2017) and Pathak et al. (2020) but they considered it as insignificant from consumers' perspective. Minimal darkening of color after plasma treatment was also noticed in CAP treated strawberries, apples, cucumbers and carrots (Wang et al., 2012; Misra et al., 2014; Baier, Ehlbeck, Knorr, Herppich and Schlüter, 2015). We speculate that the darkening of the berry color was attributed to CAP-induced loss of moisture and melting of the epicuticular surface wax on the surface of the raspberries. Alternatively, reactions between fatty acid methyl esters in epicuticular wax and plasma reactive species may have induced lipid oxidation resulting in greenish and yellowish hues in raspberries. This assumption was supported by study of Hamre, Lie, and Sandnes (2003) who found that the increase of lipid oxidation was correlated with the decrease of redness value (−a*). It appears that different cold plasma setups and experimental conditions have the potential to produce different effects on plant molecules and induce heterogenous fruit color changes.

5. Conclusion

The present study investigated inactivation efficacy and mechanism of a pulsed corona discharge system on enteric viruses attached to raspberries. Obtained results clearly showed that both MNV and HAV can be strongly inactivated and reduced >4 $\log_{10}$ in <5 and 10 min of exposure by PCDP, respectively. The main mechanism of virus inactivation was denaturation of capsid proteins by non-charged reactive species (ozone and NO_2) resulting into forceful penetration into viral particles and subsequent inactivation of viral genome. Overall, this

study developed a highly efficient and industry-acceptable strategy for inactivation of virus on raspberries having potential as a mean of improving the microbiological safety of fruits without compromising sensory attributes. Feasibility for scale-up of this technology to pilot and commercial scales for decontamination of foodborne viruses on fresh and frozen berry fruit will be the focus of our future work.

Declaration of Competing Interest

None.

Data availability

No data was used for the research described in the article.

Acknowledgement

This study was supported by the Ministry of Education, Science and Technological Development of the Republic of Serbia, according to the provisions of the Contract on research financing in 2021 (No 451-03-9/2021-14/200050 dated 05.02.2021). Putnik P. wish to thank Croatian Science Foundation for the funding of the project "Hurdle Technology and 3D Printing for Sustainable Fruit Juice Processing and Preservation;" IP-2019-04-2105. Velebit B. is thankful for the help provided by Dr. Aleksandra Korać (Faculty of Biology, University of Belgrade) in TEM imaging.

References

Aboubakr, H. A., Mor, S. K., Higgins, L., Armien, A., Youssef, M. M., Bruggeman, P. J., & Goyal, S. M. (2018). Cold argon-oxygen plasma species oxidize and disintegrate capsid protein of feline calicivirus. *PLoS One, 13*(3), Article e0194618. https://doi.org/10.1371/journal.pone.0194618

Aboubakr, H. A., Sampedro Parra, F., Collins, J., Bruggeman, P., & Goyal, S. M. (2020). In situ inactivation of human norovirus GII.4 by cold plasma: Ethidium monoazide (EMA)-coupled RT-qPCR underestimates virus reduction and fecal material suppresses inactivation. *Food Microbiology, 85*, Article 103307. https://doi.org/10.1016/j.fm.2019.103307

Ahlfeld, B., Li, Y., Boulaaba, A., Binder, A., Schotte, U., Zimmermann, J. L., … Klein, G. (2015). Inactivation of a foodborne Norovirus outbreak strain with nonthermal atmospheric pressure plasma. *mBio, 6*(1). https://doi.org/10.1128/mbio.02300-14

Ahmed, H., Maunula, L., & Korhonen, J. (2020). Reduction of Norovirus in foods by nonthermal treatments: A review. *Journal of Food Protection, 83*(12), 2053–2073. https://doi.org/10.4315/jfp-20-177

Alekseev, O., Donovan, K., Limonnik, V., & Azizkhan-Clifford, J. (2014). Nonthermal dielectric barrier discharge (DBD) plasma suppresses herpes simplex virus type 1 (HSV-1) replication in corneal epithelium. *Translational Vision Science & Technology, 3*(2), 2. https://doi.org/10.1167/tvst.3.2.2

Anttonen, M. J., & Karjalainen, R. O. (2005). Environmental and genetic variation of phenolic compounds in red raspberry. *Journal of Food Composition and Analysis, 18*(8), 759–769. https://doi.org/10.1016/j.jfca.2004.11.003

Araud, E., DiCaprio, E., Ma, Y., Lou, F., Gao, Y., Kingsley, D., … Li, J. (2016). Thermal inactivation of enteric viruses and bioaccumulation of enteric foodborne viruses in live oysters (Crassostrea virginica). *Applied and Environmental Microbiology, 82*(7), 2086–2099. https://doi.org/10.1128/aem.03573-15

Bae, S.-C., Park, S. Y., Choe, W., & Ha, S.-D. (2015). Inactivation of murine norovirus-1 and hepatitis A virus on fresh meats by atmospheric pressure plasma jets. *Food Research International, 76*, 342–347. https://doi.org/10.1016/j.foodres.2015.06.039

Baier, M., Ehlbeck, J., Knorr, D., Herppich, W. B., & Schlüter, O. (2015). Impact of plasma processed air (PPA) on quality parameters of fresh produce. *Postharvest Biology and Technology, 100*, 120–126. https://doi.org/10.1016/j.postharvbio.2014.09.015

Bidawid, S., Farber, J. M., Sattar, S. A., & Hayward, S. (2000). Heat inactivation of hepatitis A virus in dairy foods. *Journal of Food Protection, 63*(4), 522–528. https://doi.org/10.4315/0362-028x-63.4.522

Bozkurt, H., D'Souza, D. H., & Davidson, P. M. (2015a). Thermal inactivation of foodborne enteric viruses and their viral surrogates in foods. *Journal of Food Protection, 78*, 1597–1617. https://doi.org/10.4315/0362-028X.JFP-14-487

Bozkurt, H., D'Souza, D. H., & Davidson, P. M. (2015b). Thermal inactivation kinetics of human Norovirus surrogates and hepatitis A virus in Turkey deli meat. *Applied and Environmental Microbiology, 81*(14), 4850–4859. https://doi.org/10.1128/AEM.00874-15

Bunz, O., Mese, K., Zhang, W., Piwowarczyk, A., & Ehrhardt, A. (2018). Effect of cold atmospheric plasma (CAP) on human adenoviruses is adenovirus type-dependent. *PLoS One, 13*(10), Article e0202352. https://doi.org/10.1371/journal.pone.0202352

Butot, S., Putallaz, T., & Sánchez, G. (2008). Effects of sanitation, freezing and frozen storage on enteric viruses in berries and herbs. *International journal of food microbiology, 126*(1–2), 30–35. https://doi.org/10.1016/j.ijfoodmicro.2008.04.033

Capelli, F., Tappi, S., Gritti, T., de Aguiar Saldanha Pinheiro, A. C., Laurita, R., Tylewicz, U., … Rocculi, P. (2021). Decontamination of food packages from SARS-CoV-2 RNA with a cold plasma-assisted system. *Applied Sciences, 11*(9), 4177. https://doi.org/10.3390/app11094177

Cardemil, C. V., Parashar, U. D., & Hall, A. J. (2017). Norovirus infection in older adults: Epidemiology, risk factors, and opportunities for prevention and control. *Infectious Disease Clinics of North America, 31*(4), 839–870. https://doi.org/10.1016/j.idc.2017.07.012

CDC. (2021). Global Burden of Norovirus and Prospects for Vaccine Development. https://www.cdc.gov/norovirus/downloads/global-burden-report.pdf.

Cerf, O. (1977). A review tailing of survival curves of bacterial spores. *Journal of Applied Bacteriology, 42*(1), 1–19. https://doi.org/10.1111/j.1365-2672.1977.tb00665.x

Choi, M.-S., Jeon, E. B., Kim, J. Y., Choi, E. H., Lim, J. S., Choi, J., … Park, S. Y. (2020a). Virucidal effects of dielectric barrier discharge plasma on human Norovirus infectivity in fresh oysters (Crassostrea gigas). *Foods, 9*(12), 1731. https://doi.org/10.3390/foods9121731

Choi, M.-S., Jeon, E. B., Kim, J. Y., Choi, E. H., Lim, J. S., Choi, J., & Park, S. Y. (2020b). Impact of non-thermal dielectric barrier discharge plasma on Staphylococcus aureus and Bacillus cereus and quality of dried blackmouth angler (Lophiomus setigerus). *Journal of Food Engineering, 278*, Article 109952. https://doi.org/10.1016/j.jfoodeng.2020.109952

Codex Alimentarius. (2012). *CAC/GL 79-2012 Guidelines on the Application of General Principles of Food Hygiene to the Control of Viruses in Food, (p. 13)*. Rome: Codex Committee on Food Hygiene.

Dewey-Mattia, D., Manikonda, K., Hall, A. J., Wise, M. E., & Crowe, S. J. (2018). Surveillance for foodborne disease outbreaks — United States, 2009–2015. *MMWR Surveillance Summaries, 67*(10), 1–11. https://doi.org/10.15585/mmwr.ss6710a1

EC (European Commission). (2014). Plasma Gas Technique as Electronic Preservation Practice of Organic Food and Feed, EGTOP/2014, Directorate-General for Agriculture and Rural Development, Directorate, B. Multilateral Relations, Quality Policy, B. 4. Organics, Expert Group for Technical Advice on Organic Production EGTOP, Final Report on Food (III). Available online: https://ec.europa.eu/agriculture/organic/sites/orgfarming/files/docs/body/egtop-final-report-food-iii_en.pdf/.

EFSA. (2021). The European Union one health 2020 Zoonoses report. *EFSA Journal, 19*(12). https://doi.org/10.2903/j.efsa.2021.6971

Filipić, A., Gutierrez-Aguirre, I., Primc, G., Mozetič, M., & Dobnik, D. (2020). Cold plasma, a new Hope in the field of virus inactivation. *Trends in Biotechnology, 38*(11), 1278–1291. https://doi.org/10.1016/j.tibtech.2020.04.003

Fuentes, C., Pérez-Rodríguez, F. J., Sabrià, A., Beguiristain, N., Pintó, R. M., Guix, S., & Bosch, A. (2021). Inactivation of hepatitis A virus and human Norovirus in clams subjected to heat treatment. *Frontiers in Microbiology, 11*. https://doi.org/10.3389/fmicb.2020.578328

Geeraerd, A. H., Valdramidis, V. P., & Van Impe, J. F. (2005). GInaFiT, a freeware tool to assess non-log-linear microbial survivor curves. *International Journal of Food Microbiology, 102*(1), 95–105. https://doi.org/10.1016/j.ijfoodmicro.2004.11.038

Gonzalez-Hernandez, M. B., Bragazzi Cunha, J., & Wobus, C. E. (2012). Plaque assay for murine Norovirus. *Journal of Visualized Experiments, 66*. https://doi.org/10.3791/4297

Gosert, R., Egger, D., & Bienz, K. (2000). A cytopathic and a cell culture adapted hepatitis A virus strain differ in cell killing but not in intracellular membrane rearrangements. *Virology, 266*(1), 157–169. https://doi.org/10.1006/viro.1999.0070

Griffiths, D. W., Robertson, G. W., Shepherd, T., Birch, A. N. E., Gordon, S. C., & Woodford, J. A. T. (2000). A comparison of the composition of epicuticular wax from red raspberry (Rubus idaeus L.) and hawthorn (Crataegus monogyna Jacq.) flowers. *Phytochemistry, 55*(2), 111–116. https://doi.org/10.1016/s0031-9422(00)00250-8

Hamre, K., Lie, Ø., & Sandnes, K. (2003). Development of lipid oxidation and flesh colour in frozen stored fillets of Norwegian spring-spawning herring (Clupea harengus L.). effects of treatment with ascorbic acid. *Food Chemistry, 82*(3), 447–453. https://doi.org/10.1016/s0308-8146(03)00070-0

Hewitt, J., Leonard, M., Greening, G. E., & Lewis, G. D. (2011). Influence of wastewater treatment process and the population size on human virus profiles in wastewater. *Water Research, 45*(18), 6267–6276. https://doi.org/10.1016/j.watres.2011.09.029

Jiang, X., Kanda, T., Wu, S., Nakamoto, S., Saito, K., Shirasawa, H., … Yokosuka, O. (2014). Suppression of La antigen exerts potential antiviral effects against hepatitis A virus. *PLoS One, 9*(7), Article e101993. https://doi.org/10.1371/journal.pone.0101993

Kitajima, M., Oka, T., Takagi, H., Tohya, Y., Katayama, H., Takeda, N., & Katayama, K. (2010). Development and application of a broadly reactive real-time reverse transcription-PCR assay for detection of murine noroviruses. *Journal of Virological Methods, 169*(2), 269–273. https://doi.org/10.1016/j.jviromet.2010.07.018

Kuehni, R. G. (1976). Color-tolerance data and the tentative CIE 1976 L*a*b* formula. *Journal of the Optical Society of America, 66*(5), 497. https://doi.org/10.1364/josa.66.000497

Lacombe, A., Niemira, B. A., Gurtler, J. B., Fan, X., Sites, J., Boyd, G., & Chen, H. (2015). Atmospheric cold plasma inactivation of aerobic microorganisms on blueberries and effects on quality attributes. *Food Microbiology, 46*, 479–484. https://doi.org/10.1016/j.fm.2014.09.010

Lacombe, A., Niemira, B. A., Gurtler, J. B., Sites, J., Boyd, G., Kingsley, D. H., … Chen, H. (2017). Nonthermal inactivation of norovirus surrogates on blueberries using atmospheric cold plasma. *Food Microbiology, 63*, 1–5. https://doi.org/10.1016/j.fm.2016.10.030

Laroussi, M. (2020). Cold plasma in medicine and healthcare: The new frontier in low temperature plasma applications. *Frontiers in Physics, 8*. https://doi.org/10.3389/fphy.2020.00074

Liao, X., Liu, D., Xiang, Q., Ahn, J., Chen, S., Ye, X., & Ding, T. (2017). Inactivation mechanisms of non-thermal plasma on microbes: A review. *Food Control, 75*, 83–91. https://doi.org/10.1016/j.foodcont.2016.12.021

Lu, X., & Laroussi, M. (2006). Dynamics of an atmospheric pressure plasma plume generated by submicrosecond voltage pulses. *Journal of Applied Physics, 100*(6), Article 063302. https://doi.org/10.1063/1.2349475

Misra, N. N., Patil, S., Moiseev, T., Bourke, P., Mosnier, J. P., Keener, K. M., & Cullen, P. J. (2014). In-package atmospheric pressure cold plasma treatment of strawberries. *Journal of Food Engineering, 125*, 131–138. https://doi.org/10.1016/j.jfoodeng.2013.10.023

Mohamed, H., Nayak, G., Rendine, N., Wigdahl, B., Krebs, F. C., Bruggeman, P. J., & Miller, V. (2021). Non-thermal plasma as a novel strategy for treating or preventing viral infection and associated disease. *Frontiers in Physics, 9*. https://doi.org/10.3389/fphy.2021.683118

Moldgy, A., Nayak, G., Aboubakr, H. A., Goyal, S. M., & Bruggeman, P. J. (2020). Inactivation of virus and bacteria using cold atmospheric pressure air plasmas and the role of reactive nitrogen species. *Journal of Physics D: Applied Physics, 53*(43), Article 434004. https://doi.org/10.1088/1361-6463/aba066

Nasheri, N., Harlow, J., Chen, A., Corneau, N., & Bidawid, S. (2021). Survival and inactivation by advanced oxidative process of foodborne viruses in model low-moisture foods. *Food and Environmental Virology, 13*(1), 107–116. https://doi.org/10.1007/s12560-020-09457-7

Niemira, B. A. (2012). Cold plasma decontamination of foods. *Annual Review of Food Science and Technology, 3*, 125–142. https://doi.org/10.1146/annurev-food-022811-101132

Obón, J. M., Castellar, M. R., Alacid, M., & Fernández-López, J. A. (2009). Production of a red–purple food colorant from Opuntia stricta fruits by spray drying and its application in food model systems. *Journal of Food Engineering, 90*(4), 471–479. https://doi.org/10.1016/j.jfoodeng.2008.07.013

O'Connor, N., Cahill, O., Daniels, S., Galvin, S., & Humphreys, H. (2014). Cold atmospheric pressure plasma and decontamination. Can it contribute to preventing hospital-acquired infections? *Journal of Hospital Infection, 88*(2), 59–65. https://doi.org/10.1016/j.jhin.2014.06.015

Ohfuji, S., Kondo, K., Ito, K., Kase, T., Maeda, A., Fukushima, W., … Kano, M. (2019). Nationwide epidemiologic study of norovirus-related hospitalization among Japanese older adults. *BMC Infectious Diseases, 19*(1). https://doi.org/10.1186/s12879-019-4007-2

Pathak, N., Grossi Bovi, G., Limnaios, A., Fröhling, A., Brincat, J., Taoukis, P., … Schlüter, O. (2020). Impact of cold atmospheric pressure plasma processing on storage of blueberries. *Journal of Food Processing and Preservation, 44*(8). https://doi.org/10.1111/jfpp.14581

Persson, S., Alm, E., Karlsson, M., Enkirch, T., Norder, H., Eriksson, R., … Ellström, P. (2021). A new assay for quantitative detection of hepatitis A virus. *Journal of virological methods, 288*, 114010. https://doi.org/10.1016/j.jviromet.2020.114010

Persson, S., Karlsson, M., Borsch-Reniers, H., Ellström, P., Eriksson, R., & Simonsson, M. (2019). Missing the match might not cost you the game: Primer-template mismatches studied in different hepatitis A virus variants. *Food and Environmental Virology, 11*(3), 297–308. https://doi.org/10.1007/s12560-019-09387-z

Pexara, A., & Govaris, A. (2020). Foodborne viruses and innovative non-thermal food-processing technologies. *Foods, 9*(11), 1520. https://doi.org/10.3390/foods9111520

Pradeep, P., & Chulkyoon, M. (2016). Non-thermal plasmas (NTPs) for inactivation of viruses in abiotic environment. *Research Journal of Biotechnology, 11*(6), 91–96.

Randazzo, W., Khezri, M., Ollivier, J., Le Guyader, F. S., Rodríguez-Díaz, J., Aznar, R., & Sánchez, G. (2018). Optimization of PMAxx pretreatment to distinguish between human norovirus with intact and altered capsids in shellfish and sewage samples. *International Journal of Food Microbiology, 266*, 1–7. https://doi.org/10.1016/j.ijfoodmicro.2017.11.011

Randazzo, W., López-Gálvez, F., Allende, A., Aznar, R., & Sánchez, G. (2016). Evaluation of viability PCR performance for assessing norovirus infectivity in fresh-cut vegetables and irrigation water. *International Journal of Food Microbiology, 229*, 1–6. https://doi.org/10.1016/j.ijfoodmicro.2016.04.010

Rutjes, S. A., van den Berg, H. H., Lodder, W. J., & de Roda Husman, A. M. (2006). Real-time detection of noroviruses in surface water by use of a broadly reactive nucleic acid sequence-based amplification assay. *Applied and Environmental Microbiology, 72*(8), 5349–5358. https://doi.org/10.1128/AEM.00751-06

Ryu, W.-S. (2017). Other positive-Strand RNA viruses. *Molecular Virology of Human Pathogenic Viruses*, 177–184. https://doi.org/10.1016/b978-0-12-800838-6.00013-8

Sánchez, G., & Bosch, A. (2016). Survival of enteric viruses in the environment and food. *Viruses in Foods*, 367–392. https://doi.org/10.1007/978-3-319-30723-7_13

Sarangapani, C., O'Toole, G., Cullen, P. J., & Bourke, P. (2017). Atmospheric cold plasma dissipation efficiency of agrochemicals on blueberries. *Innovative Food Science & Emerging Technologies, 44*, 235–241. https://doi.org/10.1016/j.ifset.2017.02.012

Severi, E., Verhoef, L., Thornton, L., Guzman-Herrador, B. R., Faber, M., Sundqvist, L., … Rizzo, C. (2015). Large and prolonged food-borne multistate hepatitis A outbreak in Europe associated with consumption of frozen berries, 2013 to 2014. *Eurosurveillance, 20*(29). https://doi.org/10.2807/1560-7917.es2015.20.29.21192

Shimizu, T., Sakiyama, Y., Graves, D. B., Zimmermann, J. L., & Morfill, G. E. (2012). The dynamics of ozone generation and mode transition in air surface micro-discharge plasma at atmospheric pressure. *New Journal of Physics, 14*(10), Article 103028. https://doi.org/10.1088/1367-2630/14/10/103028

Simoncelli, E., Schulpen, J., Barletta, F., Laurita, R., Colombo, V., Nikiforov, A., & Gherardi, M. (2019). UV–VIS optical spectroscopy investigation on the kinetics of long-lived RONS produced by a surface DBD plasma source. *Plasma Sources Science and Technology, 28*(9), Article 095015. https://doi.org/10.1088/1361-6595/ab3c36

Song, K., Wang, H., Jiao, Z., Qu, G., Chen, W., Wang, G., … Ling, F. (2022). Inactivation efficacy and mechanism of pulsed corona discharge plasma on virus in water. *Journal of Hazardous Materials, 422*, Article 126906. https://doi.org/10.1016/j.jhazmat.2021.126906

Starek, A., Sagan, A., Andrejko, D., Chudzik, B., Kobus, Z., Kwiatkowski, M., … Pawłat, J. (2020). Possibility to extend the shelf life of NFC tomato juice using cold atmospheric pressure plasma. *Scientific Reports, 10*(1). https://doi.org/10.1038/s41598-020-77977-0

Tavoschi, L., Severi, E., Niskanen, T., Boelaert, F., Rizzi, V., Liebana, E., … Coulombier, D. (2015). Food-borne diseases associated with frozen berries consumption: A historical perspective, European Union, 1983 to 2013. *Eurosurveillance, 20*(29). https://doi.org/10.2807/1560-7917.es2015.20.29.21193

Thebault, A., Teunis, P. F. M., Le Pendu, J., Le Guyader, F. S., & Denis, J.-B. (2013). Infectivity of GI and GII noroviruses established from oyster related outbreaks. *Epidemics, 5*(2), 98–110. https://doi.org/10.1016/j.epidem.2012.12.004

Topping, J. R., Schnerr, H., Haines, J., Scott, M., Carter, M. J., Willcocks, M. M., … Knight, A. I. (2009). Temperature inactivation of feline calicivirus vaccine strain FCV F-9 in comparison with human noroviruses using an RNA exposure assay and reverse transcribed quantitative real-time polymerase chain reaction-A novel method for predicting virus infectivity. *Journal of Virological Methods, 156*(1–2), 89–95. https://doi.org/10.1016/j.jviromet.2008.10.024

Tuladhar, E., Bouwknegt, M., Zwietering, M. H., Koopmans, M., & Duizer, E. (2012). Thermal stability of structurally different viruses with proven or potential relevance to food safety. *Journal of Applied Microbiology, 112*(5), 1050–1057. https://doi.org/10.1111/j.1365-2672.2012.05282.x

Wang, R. X., Nian, W. F., Wu, H. Y., Feng, H. Q., Zhang, K., Zhang, J., … Fang, J. (2012). Atmospheric-pressure cold plasma treatment of contaminated fresh fruit and vegetable slices: Inactivation and physiochemical properties evaluation. *The European Physical Journal D, 66*(10). https://doi.org/10.1140/epjd/e2012-30053-1

Weber, C. A., Perkins-Veazie, P., Moore, P. P., & Howard, L. (2008). Variability of antioxidant content in raspberry Germplasm. *Acta Horticulturae, 777*, 493–498. https://doi.org/10.17660/actahortic.2008.777.75

Weiss, M., Daeschlein, G., Kramer, A., Burchardt, M., Brucker, S., Wallwiener, D., & Stope, M. B. (2017). Virucide properties of cold atmospheric plasma for future clinical applications. *Journal of Medical Virology, 89*(6), 952–959. https://doi.org/10.1002/jmv.24701

Weltmann, K., Kindel, E., von Woedtke, T., Hähnel, M., Stieber, M., & Brandenburg, R. (2010). Atmospheric-pressure plasma sources: Prospective tools for plasma medicine. *Pure and Applied Chemistry, 82*(6), 1223–1237. https://doi.org/10.1351/PAC-CON-09-10-35

World Health Organization. (2019). Food safety. https://www.who.int/news-room/fact-sheets/detail/food-safety (accessed 01.03.2020).

Wu, Y., Liang, Y., Wei, K., Li, W., Yao, M., Zhang, J., & Grinshpun, S. A. (2015). MS2 virus inactivation by atmospheric-pressure cold plasma using different gas carriers and power levels. *Applied and Environmental Microbiology, 81*(3), 996–1002. https://doi.org/10.1128/aem.03322-14

Xin, Q., Li, Z., Lei, L., & Yang, B. (2016). Inactivation of Bacteria in oil field injected water by a pulsed plasma discharge process. *Plasma Science and Technology, 18*(9), 943–949. https://doi.org/10.1088/1009-0630/18/9/11